Journal of Alloys and Compounds 480 (2009) 839–842

Contents lists available at ScienceDirect

Journal of Alloys and Compounds

journal homepage: www.elsevier.com/locate/jallcom

Growth and spectral properties of Nd^{3+}-doped $Li_3Ba_2Ln_3(MoO_4)$ (Ln = La, Gd) crystals

Mingjun Song[a,b], Lizhen Zhang[a], Guofu Wang[a,*]

[a] State Key Laboratory of Structural Chemistry, Fujian Institute of Research on the Structure of Matter, The Chinese Academy of Sciences, Fuzhou, Fujian 350002, China
[b] Graduate School of the Chinese Academy of Sciences, Beijing 100039, China

ARTICLE INFO

Article history:
Received 24 November 2008
Received in revised form 12 February 2009
Accepted 14 February 2009
Available online 4 March 2009

Keywords:
Crystal growth
Luminescence
Photoelectron spectroscopies

ABSTRACT

This paper reports the growth and spectroscopic properties of Nd^{3+}:$Li_3Ba_2Ln_3(MoO_4)_8$ (Ln = La, Gd) crystals. Nd^{3+}:$Li_3Ba_2Gd_3(MoO_4)_8$ crystal with dimensions of 40 mm × 40 mm × 10 mm and Nd^{3+}:$Li_3Ba_2La_3(MoO_4)_8$ crystal with dimensions of 15 mm × 28 mm × 8.0 mm have been successfully grown from a flux of Li_2MoO_4. The spectroscopic properties of both crystals were investigated. The results show that Nd^{3+}:$Li_3Ba_2Ln_3(MoO_4)_8$ (Ln = Gd, La) crystals may be regarded as a potential solid-state laser host material for diode laser pumping.

1. Introduction

With the development of diode-pumped solid-state lasers, the research on new laser materials has been gained much interest [1–22]. Some Nd^{3+}-doped molybdate crystals have been attracted attention because they have high-quantum efficiency [22–24]. The compound $Li_3Ba_2Ln_3(MoO_4)_8$ (Ln = La–Lu, Y), which was discovered by Klevtsova et al. [25], belongs to the monoclinic system with space group *C*2/*c*. In previous work, the efficient laser performance has already been obtained in Nd^{3+}-doped $Li_3Ba_2Gd_3(MoO_4)_8$ [26,27]. However, to our knowledge, the detailed growth method and the spectroscopic analysis of Nd^{3+}:$Li_3Ba_2Gd_3(MoO_4)_8$ have not yet been reported. Recently, we have reported the growth and spectral properties of Nd^{3+}-doped $Li_3Ba_2Y_3(MoO_4)_8$ [28]. Therefore, this paper further reports the growth and spectroscopic characteristics of Nd^{3+}-doped $Li_3Ba_2Ln_3(MoO_4)_8$ (Ln = Gd, La) crystals.

2. Crystal growth

Since $Li_3Ba_2Ln_3(MoO_4)_8$ (Ln = La, Gd) compound melts incongruently, it is only grown by the flux method. $Li_3Ba_2Ln_3(MoO_4)_8$ (Ln = La, Gd) crystals were grown from a flux of Li_2MoO_4 by the top seeded solution growth (TSSG) method. The chemicals used were Li_2CO_3, $BaCO_3$, Gd_2O_3, La_2O_3, Nd_2O_3 and MoO_3 with purity of 99.99%. The stoichiometric amounts of raw materials were weighed according to the following chemical reaction:

$$3Li_2CO_3 + 2BaCO_3 + 6(1-x)Ln_2O_3 + 6xNd_2O_3 + 16MoO_3 = 2Li_3Ba_2Ln_{(3-3x)}Nd_{3x}(MoO_4)_8 + CO_2\uparrow \quad (1)$$

After grinding and extruding to form pieces, the samples were placed in a platinum crucible and held at 900 °C for 3 days, repeating once again to assure adequate solid-state reaction. The growth of $Li_3Ba_2Ln_3(MoO_4)_8$ (Ln = La, Gd) crystals were carried out in a vertical tubular furnace with nickel–chrome wire as heating element. A temperature controller of AL-708 was controlled the furnace temperature and cooling rate. $Li_3Ba_2Ln_3(MoO_4)_8$ (Ln = La, Gd) crystals were grown from the flux of Li_2MoO_4 by TSSG method. The 4 at.% Nd^{3+}-doped $Li_3Ba_2La_3(MoO_4)_8$ and 5 at.% Nd^{3+}-doped $Li_3Ba_2La_3(MoO_4)_8$ and Li_2MoO_4 were weighed, respectively. The molar ratio of $Li_3Ba_2Ln_3(MoO_4)_8$:Li_2MoO_4 was 1:3. The weighed about 200 g raw materials were placed into the platinum crucible. The procedure of crystal growth was as following: the fully charged crucibles were placed into the furnace and heated up to 950 °C. The solution was held at 950 °C for 2 days to make the solution melt completely and homogeneously. The crystals were first grown by spontaneous nucleation using a platinum wire as seed. The solution temperature was cooled down to 800 °C at a cooling rate of 20 °C/day. Then, the obtained polycrystals was drawn out from the solution and cooled down to room temperature. Secondly, a seed cut from the as-grown polycrystals was used to grow large single crystal. After repeating the seeding and adjusting the heating power of the furnace, the seed contacted the surface of the solution. The crystals were grown at a cooling rate of 1 °C/day and a rotating rate of 9 rpm. After a period of about 30 days, the crystals were drawn out of

* Corresponding author. Tel.: +86 591 83714636; fax: +86 591 83714636.
E-mail address: wgf@fjirsm.ac.cn (G. Wang).

0925-8388/$ – see front matter © 2009 Elsevier B.V. All rights reserved.
doi:10.1016/j.jallcom.2009.02.082

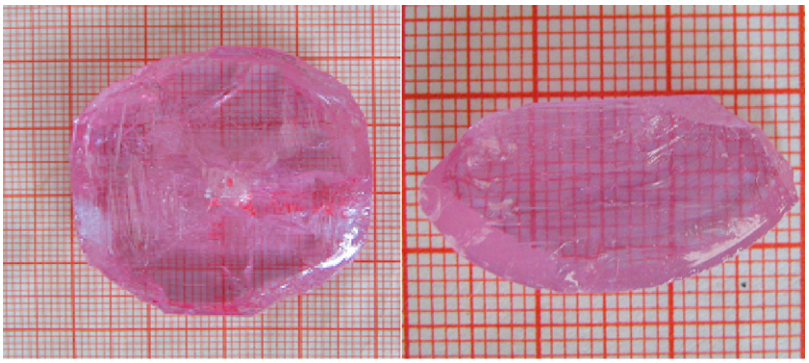

Fig. 1. Crystals grown by TSSG method: (a) Nd^{3+}:$Li_3Ba_2Gd_3(MoO_4)_8$ crystal; (b) Nd^{3+}:$Li_3Ba_2La_3(MoO_4)_8$ crystal.

the surface of the solution and cooled down to room temperature at a rate of 25 °C/h. Nd^{3+}:$Li_3Ba_2Gd_3(MoO_4)_8$ crystal with dimensions of 40 mm × 40 mm × 10 mm and Nd^{3+}:$Li_3Ba_2La_3(MoO_4)_8$ crystal with dimensions of 15 mm × 28 mm × 8.0 mm were obtained, as shown in Fig. 1. The compositions of the grown crystals were measured by the ICP-AES analysis method. The ICP-AES results are listed in Table 1. The ICP-AES results shown that the composition of Nd^{3+}:$Li_3Ba_2Ln_3(MoO_4)_8$ (Ln = Gd, La) crystals is near stoichiometric, i.e. $Li_{2.7}Ba_2Gd_{3.01}Nd_{0.09}\phi_{0.2}(MoO_4)_8$ and $Li_{2.63}Ba_2La_{2.83}Nd_{0.12}\phi_{0.42}(MoO_4)_8$ (where ϕ represents the vacancies in the cation site). Previors investigation has shown that the Li deficiency and excess incorporation of trivalent ions result in the vacancies in the molybdate crystals [29,30]. Therefore, ICP-AES results can confirm that the grown crystals belong to $Nd3^{+}$:$Li_3Ba_2Gd_3(MoO_4)_8$ and Nd^{3+}:$Li_3Ba_2La_3(MoO_4)_8$ crystals, respectively.

3. Spectral properties

The samples with dimension 12.1 mm × 8.4 mm × 1.83 mm for Nd^{3+}:$Li_3Ba_2Gd_3(MoO_4)_8$ and 11.2 mm × 8.1 mm × 1.6 mm for Nd^{3+}:$Li_3Ba_2La_3(MoO_4)_8$ were cut from the as-grown crystals and polished for the spectral measurement. The absorption spectrum was recorded on a PerkinElmer UV–VIS–NIR Spectrometer (Lambda-900) in a range of 300–1000 nm at room temperature. The fluorescence spectrum and fluorescence lifetime were measured at room temperature using an Edinburgh Analytical Instruments FLS92 excited with 807 nm radiation.

Fig. 2 shows the absorption spectra of Nd^{3+}:$Li_3Ba_2Gd_3(MoO_4)_8$ and Nd^{3+}:$Li_3Ba_2La_3(MoO_4)_8$ crystals at room temperature. In both absorption spectra there are six strong absorption bands at near about 356, 524, 589, 752, 808 and 886 nm, corresponding to $4f^3$–$4f^3$ transition of Nd^{3+} ions. In the absorption spectra the most interesting is the absorption band at about 805 nm, which is closed to the emission wavelength of the diode lasers. The FWHM of absorption bands at 805 nm are 6 nm for Nd^{3+}:$Li_3Ba_2Gd_3(MoO_4)_8$ and 7 nm for Nd^{3+}:$Li_3Ba_2La_3(MoO_4)_8$ crystals, respectively. Such large FWHM is very suitable for diode laser pumping, since it is not

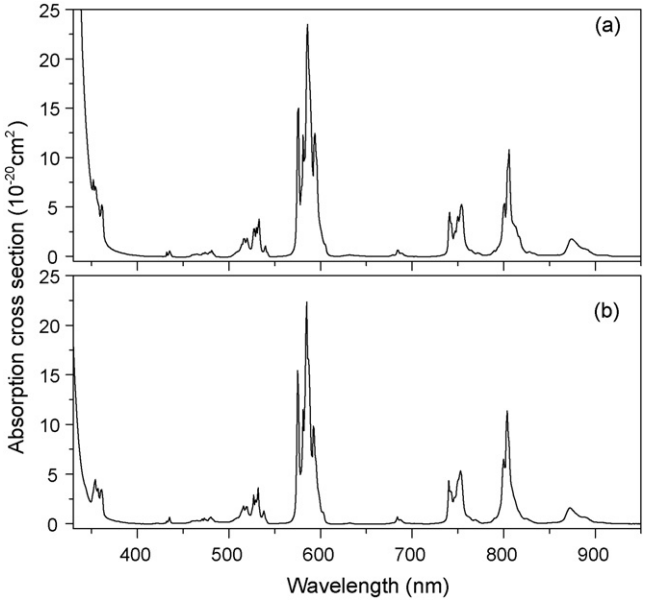

Fig. 2. Absorption spectra at room temperature: (a) Nd^{3+}:$Li_3Ba_2Gd_3(MoO_4)_8$ crystal; (b) Nd^{3+}:$Li_3Ba_2La_3(MoO_4)_8$ crystal.

crucial to temperature stability the output wavelength of diode laser. The absorption cross-sections of Nd^{3+}:$Li_3Ba_2Gd_3(MoO_4)_8$ and Nd^{3+}:$Li_3Ba_2La_3(MoO_4)_8$ crystals are 10.78 and 11.40 × 10^{-20} cm^2 at around 805 nm, respectively.

Based on the Judd–Ofelt theory [31,32], the date of absorption spectrum can be used to predict the oscillator strength parameters, radiative lifetime and radiative quantum efficiency. The calculating procedure follows those in Ref. [33]. The calculated results are listed in Tables 2 and 3.

Fig. 3 shows the fluorescence spectra of Nd^{3+}:$Li_3Ba_2Ln_3(MoO_4)_8$ (Ln = La, Gd) crystals excited with 807 nm radiation at room temperature. In the fluorescence spectra three emission bands corresponding to the $^4F_{3/2} \rightarrow {}^4I_{9/2}$, $^4I_{11/2}$ and $^4I_{13/2}$ transitions are

Table 1
The composition of Nd^{3+}:$Li_3Ba_2Ln_3(MoO_4)_8$ (Ln = Gd, La) crystals measured by the ICP-AES method.

Crystals	Nd^{3+}:$Li_3Ba_2Gd_3(MoO_4)_8$					Nd^{3+}:$Li_3Ba_2La_3(MoO_4)_8$				
	Li[a]	Ba[a]	Gd[a]	Nd[a]	Gd + Nd[a]	Li[a]	Ba[a]	La[a]	Nd[a]	La + Nd[a]
ICP result (wt.%)	0.83	12.24	21.25	0.603	21.85	0.92	13.9	19.2	0.87	20.07
Atom	0.12	0.089	0.134	0.004	0.138	0.133	0.101	0.138	0.006	0.144
Ratio of atom	2.7	2	3.01	0.09	3.1	2.63	2	2.83	0.12	2.95
Error (%)	−10	0	+0.3	–	+3.3	−9.0	0	−5.6	–	−1.7

[a] Ions.

Table 2
The spectral parameters of Nd^{3+}:$Li_3Ba_2Ln_3(MoO_4)_8$ (Ln = Gd, La) and other Nd^{3+}-doped crystals.

Crystals	Ω_2 ($\times10^{-20}$ cm^2)	Ω_4 ($\times10^{-20}$ cm^2)	Ω_6 ($\times10^{-20}$ cm^2)	FWHM (nm)	σ_a ($\times10^{-20}$ cm^2)	σ_{em} ($\times10^{-20}$ cm^2)	τ_f (μS)	η (%)	Ref.
3.4 at.% Nd^{3+}:$Li_3Ba_2Gd_3(MoO_4)_8$	22.965	6.854	6.395	6	10.78	8.7	130	94	This Work
4.4 at.% Nd^{3+}:$Li_3Ba_2La_3(MoO_4)_8$	19.529	6.394	6.579	7	11.40	6.2	135	95	This Work
2.1 at.% Nd^{3+}:$BaGd_2(MoO_4)_4$	14.964	5.044	3.580	5	3.42	22.1	156	83	[21]
5.27 at.% Nd^{3+}:$KLa(MoO_4)_2$	18.50	4.66	4.49	5	11.38	9.7	158	93	[23]
3.0 at.% Nd^{3+}:$Gd_2(MoO_4)$	8.54	5.53	6.78	–	–	–	157	86	[24]
4.8 at.% Nd^{3+}:$Li_3Ba_2Y_3(MoO_4)_8$	22.1	7.0	6.9	6	10.64	11.6	106	95	[28]
1.5 at.% Nd^{3+}:$KGd(WO_4)_2$	12.67	10.15	7.48	–	26	34	129	92	[35,36]
4.6 at.% Nd^{3+}:$KY(WO_4)_2$	8.80	3.11	3.16	4	5.18	5.4	154	79	[37]
Nd^{3+}:$NaBi(WO_4)_2$	30.9	12.0	9.3	10	2.6	16	122	85	[38]
8.2 at.% Nd^{3+}:α-$LaSc_3(BO_3)_4$	3.92	4.41	4.14	–	–	1.3	225	49.8	[41]
4.0 at.% Nd^{3+}:$GdAl_3(BO_3)_4$	1.89	2.55	4.95	9	4.3	6.3	293	18.7	[33,42]

Table 3
The transition probabilities and branch ratios for the $^4F_{3/2} \rightarrow {}^4I_j$ transitions of Nd^{3+}:$Li_3Ba_2Ln_3(MoO_4)_8$ (Ln = Gd, La) crystals.

Transition	Nd^{3+}:$Li_3Ba_2Gd_3(MoO_4)_8$		Nd^{3+}:$Li_3Ba_2La_3(MoO_4)_8$	
	β	A (S^{-1})	β	A (S^{-1})
$^4F_{3/2} \rightarrow {}^4I_{9/2}$	0.439	3190	0.439	3190
$^4F_{3/2} \rightarrow {}^4I_{11/2}$	0.467	3392	0.467	3392
$^4F_{3/2} \rightarrow {}^4I_{13/2}$	0.090	651	0.090	651
$^4F_{3/2} \rightarrow {}^4I_{15/2}$	0.005	34	0.005	34

observed at 860–940, 1036–1120, 1320–1405 nm. The emission cross-section σ_{em} of both crystals can be calculated using the following formula [34]:

$$\sigma_{em}(\lambda) = \beta \frac{\lambda^2}{4\pi^2 n^2 \tau_f \Delta\nu} \quad (2)$$

where λ is emission wavelength, τ_f is the fluorescence lifetime, $\Delta\nu$ is the half-width frequency and n is the refractive index which is estimated as 2, β is the fluorescence branch ratio which is listed in Table 3. Then emission cross-sections σ_{em} at 1.06 μm are 8.7×10^{-20} cm^2 for Nd^{3+}:$Li_3Ba_2Gd_3(MoO_4)_8$ crystal and 6.2×10^{-20} cm^2 for Nd^{3+}:$Li_3Ba_2La_3(MoO_4)_8$ crystal, respectively. The fluorescence lifetimes were measured to be 130 for Nd^{3+}:$Li_3Ba_2Gd_3(MoO_4)_8$ crystal and 135 μs for Nd^{3+}:$Li_3Ba_2La_3(MoO_4)_8$ crystal, respectively. Then, the quantum efficiency η of both crystals, where $\eta = \tau_f/\tau_{rad}$, were calculated to be 94% for Nd^{3+}:$Li_3Ba_2Gd_3(MoO_4)_8$ crystal and 95% for Nd^{3+}:$Li_3Ba_2La_3(MoO_4)_8$ crystals, respectively.

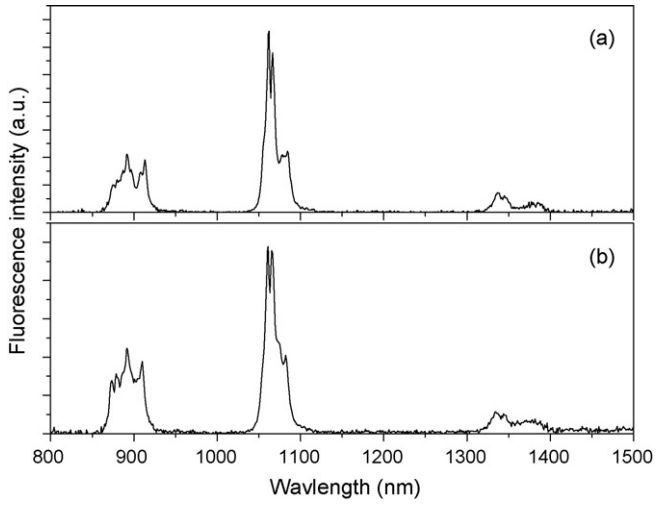

Fig. 3. Fluorescence spectra excited 807 nm radiation at room temperature: (a) Nd^{3+}:$Li_3Ba_2Gd_3(MoO_4)_8$ crystal; (b) Nd^{3+}:$Li_3Ba_2La_3(MoO_4)_8$ crystal.

4. Conclusion

Nd^{3+}:$Li_3Ba_2Gd_3(MoO_4)_8$ crystal with dimensions of 40 mm × 40 mm × 10 mm and Nd^{3+}:$Li_3Ba_2La_3(MoO_4)_8$ crystal with dimensions of 15 mm × 28 mm × 8.0 mm were successfully grown from the flux of Li_2MoO_4. The spectroscopic properties of Nd^{3+}:$Li_3Ba_2Ln_3(MoO_4)_8$ (Ln = Gd, La) crystals were investigated. In comparison with the other Nd^{3+}-doped molydbate and tungstate crystals, Nd^{3+}:$Li_3Ba_2Ln_3(MoO_4)_8$ (Ln = Gd, La) crystals have a large FWHM around 805 nm, which is suitable for diode-laser pumping. The absorption and emission cross-sections are smaller than that of Nd^{3+}:$KGd(WO_4)_2$, but larger than that of the other Nd^{3+}-doped molydbate and tungstate crystals. Both crystals have a high-fluorescence quantum efficiency as well as Nd^{3+}:$Li_3Ba_2Y_3(MoO_4)_8$ crystal (η = 95%) [28]. This phenomenon also exists in the other molydbate crystals. Such high-quantum efficiency is ascribed to the low-phonon energy of $(MoO_4)^{2-}$ groups in Nd^{3+}:$Li_3Ba_2Ln_3(MoO_4)_8$, which is generally below 1000 cm^{-1} [39,40]. In principle, the high-energy phonons usually considered to make the dominant contribution to the multiphonon relaxation from the $^4F_{3/2}$ state to the nest lower state $^4I_{15/2}$ since they can interact with electrons to conserve energy in the lowest order process. When the multiphonon nonradiative relaxation rate is generally large, it leads to the low-quantum efficiency. The phonon energy of $(MoO_4)^{2-}$ group is generally below 1000 cm^{-1} [39,40], while the phonon energy of $(BO_3)^{3-}$ in borate crystals is 1300–1400 cm^{-1} [43]. Therefore, multiphonon nonradiative relaxation rate in the molybdate crystal is generally smaller in the borate crystals, which leads high-quantum efficiency of the molybdate crystals. In conclusion, Nd^{3+}:$Li_3Ba_2Ln_3(MoO_4)_8$ (Ln = La, Gd) crystal may be regarded as a potential solid-state laser host material.

Acknowledgements

This work is supported by the National Natural Science Foundation of China (no. 60378031) and Key Project of Science and Technology of Fujian Province (2001F004), respectively.

References

[1] X.D. Xu, Z.W. Zhao, P.X. Song, J. Xu, P.Z. Deng, J. Alloys Compd. 364 (2004) 311–314.
[2] Y. Zhang, Z.B. Lin, Z.S. Hu, G.F. Wang, J. Alloys Compd. 390 (2005) 194–196.
[3] T. Bodzaiony, S.M. Kaczmarek, J. Hanuza, J. Alloys Compd. 451 (2008) 240–247.
[4] M. Dammak, S. Kammoun, R. Maalej, T. Koubaa, M. Kamoun, J. Alloys Compd. 432 (2007) 18–22.
[5] G.H. Jia, C.Y. Tu, J.F. Li, Z.J. Zhu, Z.Y. You, Y. Wang, B.C. Wu, J. Alloys Compd. 436 (2007) 341–344.
[6] R. Ternane, M. Ferid, Y. Guyot, M. Trabelsi-Ayadi, G. Boulon, J. Alloys Compd. 464 (2008) 327–331.
[7] E. Cavalli, G. Calestani, A. Belletti, E. Bovero, J. Alloys Compd. 451 (2008) 143–145.
[8] J. Pisarska, W. Ryba-Romanowski, G. Dominiak-Dzik, T. Goryczka, W.A. Pisarski, J. Alloys Compd. 451 (2008) 223–225.

[9] S. Lis, Z. Piskuła, Z. Hnatejko, J. Alloys Compd. 451 (2008) 388–394.
[10] D. Hreniak, W. Strek, P. Głuchowski, R. Fedyk, W. Łojkowski, J. Alloys Compd. 451 (2008) 549–552.
[11] C.K. Jayasankar, R. Balakrishnaiah, V. Venkatramu, A.S. Joshi, A. Speghini, M. Bettinelli, J. Alloys Compd. 451 (2008) 697–701.
[12] L. Lipinska, L. Lojko, A. Klos, S. Ganschow, R. Diduszko, W. Ryba-Romanowski, A. Pajaczkowska, J. Alloys Compd. 432 (2007) 177–182.
[13] J.M. Fan, Z.L. Zhang, L.Z. Zhang, G.F. Wang, G.F. Wang, J. Alloys Compd. 436 (2007) 252–255.
[14] N. Zhuang, Z. Lin, L. Zhang, G. Wang, Mater. Res. Innov. 11 (2007) 51–53.
[15] H. Wu, L. Zhang, Z. Lin, G. Wang, Mater. Res. Innov. 11 (2007) 31–36.
[16] B. Wei, L.Z. Zhang, Z.B. Lin, G.F. Wang, Mater. Res. Innov. 11 (2007) 144–147.
[17] B. Wei, L.Z. Zhang, Z.B. Lin, G.F. Wang, Mater. Res. Innov. 11 (2007) 154–157.
[18] S. Yu, Z.B. Lin, L.Z. Zhang, G.F. Wang, Mater. Res. Innov. 11 (2007) 177–180.
[19] Y. Zhang, Z.B. Lin, Li.Z. Zhang, G.F. Wang, Opt. Mater. 29 (2007) 543–546.
[20] X.Z. Li, Z.B. Lin, L.Z. Zhang, G.F. Wang, Opt. Mater. 29 (2007) 728–731.
[21] D. Zhao, Z.B. Lin, L.Z. Zhang, G.F. Wang, J. Phys. D: Appl. Phys. 40 (2007) 1018–1021.
[22] B. Wei, Z.B. Lin, L.Z. Zhang, G.F. Wang, J. Phys. D: Appl. Phys. 40 (2007) 2792–2796.
[23] E. Cavalli, E. Zannoni, C. Mucchino, J. Opt. Soc. Am. B 16 (1999) 1958–1965.
[24] Y.Q. Zou, X.Y. Chen, Y.D. Tang, Z.D. Luo, W.Q. Yang, Opt. Commun. 167 (1999) 99–104.
[25] R.F. Klevtsova, A.D. Vasil'ev, L.A. Glinskaya, A.D. Kruglik, N.M. Kozhevnikova, V.P. Korsun, Zh. Strukt. Khim. 33 (1992) 126–130.
[26] A. A. Demidovich, A.N. Kuzmin, G.I. Ryabtsev, L.E. Batay, A.N. Titov, in: CLEO'97, 1997 OSA Technical Digest Series, v.11, pp. 361–361.
[27] L.E. Batay, A.A. Demidovich, A.N. Kuzmin, G.I. Ryabtsev, W.S. Trek, A.N. Titov, Spectrochim. Acta A 54 (1998) 2117–2120.
[28] M.J. Song, G.J. Wang, Z.B. Lin, L.Z. Zhang, G.F. Wang, J. Cryst. Growth 308 (2007) 208–212.
[29] A. Gracía-Cortés, C. Cascales, C. Zaldo, Mater. Sci. Eng. B 146 (2008) 89–94.
[30] L.H. Brixner, J. Phys. Soc. Jpn. 38 (1975) 1218–11218.
[31] B.R. Judd, Phys. Rev. 127 (1962) 750–761.
[32] G.S. Ofelt, J. Chem. Phys. 37 (1962) 511–520.
[33] G.F. Wang, J. Opt. Soc. Am. B 18 (2001) 173–175.
[34] G. Huber, W.W. Krühler, W. Bludau, H.G. Daniemeyer, J. Appl. Phys. 46 (1975) 3580–3584.
[35] R. Moncorge, B. Chambon, J.Y. Rivorie, N. Garnier, E. Descroix, P. Laporte, H. Guillet, S. Roy, J. Mareschal, D. Pelenc, J. Doury, P. Farge, Opt. Mater. 8 (1997) 109–119.
[36] Y. Kalisky, L. Kravchik, C. Labbe, Opt. Commun. 189 (2001) 113–125.
[37] X.M. Han, G.F. Wang, J. Cryst. Growth 247 (2003) 551–554.
[38] A. Mendez-Blas, M. Rico, V. Volkov, C. Zaldo, C. Cascales, Mol. Phys. 101 (2003) 941–949.
[39] J. Hanuza, L. Labuda, J. Raman Spectrosc. 11 (1981) 231–237.
[40] E. Cavalli, C. Meschini, A. Toncelli, M. Tonelli, M. Bettinelli, J. Phys. Chem. Solids 58 (1997) 587–595.
[41] G.F. Wang, W.Z. Chen, Z.B. Lin, Z.S. Hu, Phys. Rev. B 60 (1999) 15469–15471.
[42] G.F. Wang, Z.B. Lin, Z.S. Hu, T.P.J. Han, H.G. Gallagher, J.-P.R. Wells, J. Cryst. Growth 233 (2001) 755–760.
[43] X.Y. Chen, Z.D. Luo, D. Jaque, J.J. Romero, J. Garcia Sole, Y.D. Huang, A.D. Jiang, C.Y. Tu, J. Phys.: Conden. Matter 13 (2001) 1171–1178.